

Inductance Extraction by Means of the Monte Carlo Method

G. Leonhardt, C. Hager, P. Regli and W. Fichtner

Integrated Systems Laboratory
Swiss Federal Institute of Technology
Gloriastr. 35, 8092 Zurich, Switzerland, leonhardt@iis.ee.ethz.ch

Abstract

This paper presents a novel inductance extraction procedure which is based on a Monte Carlo sampling technique. Partial inductances for static current distributions can be computed efficiently and with small memory requirements, thus enabling the treatment of large and complex three-dimensional geometries. The convergence behavior is discussed and examples are presented along with a comparison to the Fasthenry code [1].

Keywords: Inductance Extraction - Monte Carlo

Introduction

With increasing signal frequencies inductive effects of electrical interconnections in all kinds of packages become more and more important for the performance of a circuit. During the design process it is therefore of interest to have a stable, fast and accurate simulation tool which is capable of extracting self and mutual inductances of large and complicated geometries.

The formulation which is presented here is limited to static inductance extraction, i.e., the skin effect is not considered. However, the skin effect can be neglected for a large class of applications where the conductor diameter is small compared to the skin depth

$$\delta = 1/\sqrt{\mu\sigma\omega}$$

which is a measure of how deep the electromagnetic field penetrates into a conductor.

The inductance extraction procedure consists of two main steps that are quite independent of each other: 1) Computation of the current density distribution in the conductors, 2) Computation of the magnetic energies associated with the self- and mutual inductance terms.

The computation of the current density distribution is not in the main focus of this paper as it is a standard problem involving the solution of a Poisson equation. Any existing program can be used for this part. For the examples presented here, the commercial tool SOLIDIS-ISE has been used for this step. SOLIDIS-ISE is a finite element solver with efficient adaptive refinement capabilities.

The computation of the magnetic energy W from the available current density distribution is accomplished by evaluating Neumann's formula [2]:

$$W = \frac{\mu}{8\pi} \int_V \int_{V'} \frac{\vec{J}(\vec{r}) \cdot \vec{J}(\vec{r}')}{|\vec{r} - \vec{r}'|} dV' dV \quad (1)$$

by means of a Monte Carlo sampling technique. V and V' denote the volume of the conductor, r and r' are locations in these volumes.

Self Inductance

The self inductance L of a single conductor is related to the magnetic energy W by

$$W = \frac{1}{2} LI^2. \quad (2)$$

W is calculated with a sample mean Monte Carlo method [3]. For every sample the two locations r and r' are chosen randomly somewhere in the conductor in the following way: First, an element of the conductor, corresponding to the finite element of the grid used for the computation of the current density, is chosen with probability proportional to the volume of this element. After that, the location inside the selected element is chosen with constant probability density. The current density in the element is calculated from the derivative of the electric potential in the center of the element and is therefore a constant in every grid element.

Inductive Coupling

In case of multiple conductors, the mutual inductive couplings are also computed. With least computational effort current distributions in the conductors are computed for a given voltage difference between the contacts at their ends. For N conductors, N different current distributions J_i with $i = 1, \dots, N$ are computed. J_i is the current distribution for 1V voltage difference across conductor i , 0V across all other conductors. The energy computation 1 is now modified.

$$W_{ij} = \frac{\mu}{8\pi} \int_V \int_{V'} \frac{\vec{J}_i(\vec{r}) \cdot \vec{J}_j(\vec{r}')}{|\vec{r} - \vec{r}'|} dV' dV \quad (3)$$

Here W_{ij} is the potential energy of current distribution J_i in the magnetic field of current distribution J_j or vice versa and therefore $W_{ij} = W_{ji}$.

The inductive behaviour of N conductors is described with a matrix L where the diagonal entries L_{ii} are the self inductance of the conductors i , whereas the off-diagonal entries L_{ij} stand for the inductive coupling between conductors i and j . In order to use the relation between energy and inductance (2) for the multi conductor case we define current vectors I_i with $i = 1, \dots, N$. The k th element of vector I_i , i.e. I_{ik} , is the current through conductor k for current distribution J_i . The energy W_{ij} (3 in terms of inductances becomes now

$$W_{ij} = \frac{1}{2} I_i^T L I_j$$

or, when defining a current matrix I with columns I_i in matrix notation

$$W = \frac{1}{2} I^T L I \quad (4)$$

Since W is symmetric $1/2N(N+1)$ energy terms W_{ij} have to be calculated. With also I known, the inductance matrix L can be calculated by matrix inversion.

Note that this formulation also holds for conductors with more than two contacts.

Error Estimation

The computational error involved in the procedure described above is caused mainly by two different sources. One is the approximative nature of the current density obtained from the finite element computation. A second source of inaccuracy is the subsequent energy calculation by statistical means. While the accuracy of the current density calculation can be improved by refining the grid or by using higher order discretizations, the error made in the evaluation of the magnetic energy terms is dependent only on the number of samples, i.e., the number of iterations used in the Monte Carlo procedure.

The statistical error in the calculation of the magnetic energy can be estimated from the number of iterations and from the variance of the sampled values [3]. Due to the iterative nature of the Monte Carlo procedure, the sampling process can be stopped once a specified accuracy has been achieved.

Convergence

Some interesting aspects of the convergence behavior become apparent when studying geometries of different dimensionality. To demonstrate this, three example geometries have been analyzed (see Figure 1). Geometry "A" is a long conductor (1D case), "B" is a flat planar conductor (2D case), and "C" is a cube-like conductor (3D case). All geometries are in fact three-dimensional discretized objects, but the aspect ratios are chosen in such a way as to simulate the behaviour for quasi one-dimensional and quasi two-dimensional geometries. In

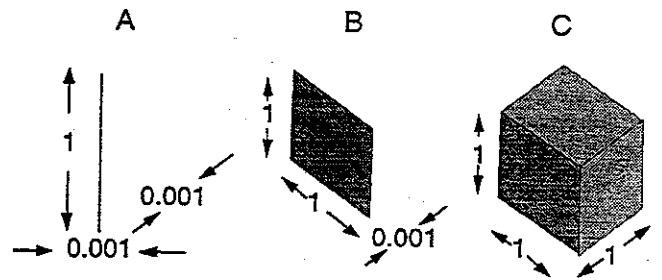


Figure 1: Geometries A, B and C for which the inductance is calculated with Monte Carlo sampling.

all three cases, a homogeneous current density in the conductor has been assumed.

In the course of the Monte Carlo sampling procedure, the integral (1) is calculated only approximately. After n iterations the value obtained for the energy $W_n \approx W$ is

$$W_n \propto \frac{1}{n} \sum_{i=1}^n \frac{1}{|r_i - r'_i|}, \quad (5)$$

which is actually an approximation for the expectation value of the inverse distance distribution. Figure 3 shows the statistical distribution and the expectation value of the inverse distance $1/|r - r'|$ for the three cases. In the three-dimensional case (case "C"), the expectation value is very close to the most probable value, i.e., to the peak of the inverse distance distribution. This distribution also has the largest peak value. The maximum of the distribution decreases in case "B" and "A", and the distance between the expectation value and the most probable value increases. This suggests that the convergence of the Monte Carlo iteration should be quickest in the 3D case. To verify this, the inductance computation has been performed according to (5) for all three cases. The convergence history is shown in Figure 2. As can be seen in the figure, fastest convergence occurs in the 3D case, as expected.

A suitable quantitative measure for convergence and error estimation is the standard deviation σ of the sampled values. The probability of an error larger than $3\sigma/\sqrt{n}$ is smaller than 1 percent. This "3 σ -criterion" is used for the calculation of the error estimate during the iteration process.

The expectation values shown in Figure 3 correspond to the inductances of the corresponding geometries. Note that the inductance of an ideal one-dimensional wire is not defined, but, as mentioned before, case "A" is not really an infinitesimally thin wire but a wire with small but finite thickness.

As a consequence of these observations, it can be concluded that the convergence rate of the Monte Carlo procedure is strongly dependent on the conductor shapes. Thin wires and thin plates will tend to have slower convergence because the expectation value and the most

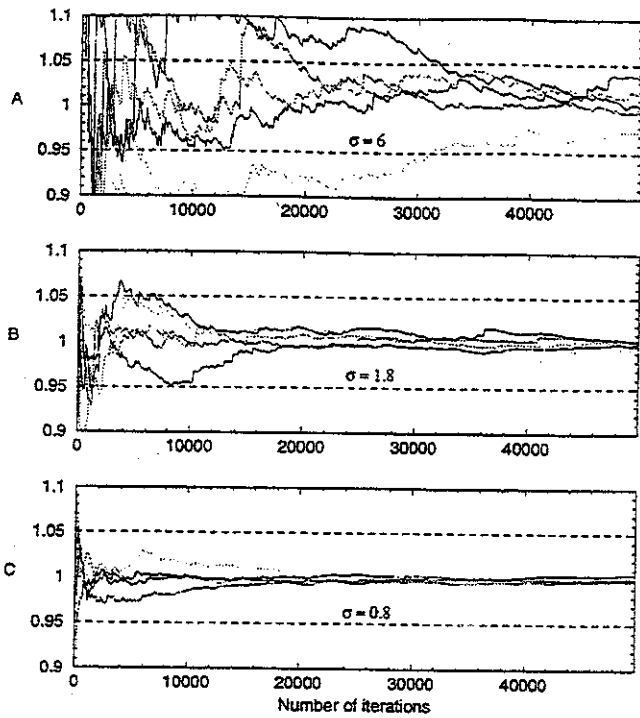


Figure 2: Running average of inductance divided by the analytical result for geometries shown in Figure 1. The standard deviation σ of the sampled normalized values is also shown.

probable value of the inverse distance distribution are not as close together as in the case of geometries that are extended equally in all three dimensions.

In addition to the influence of the geometrical shape, the convergence behavior is also strongly affected by inhomogeneities in the current density distribution.

Example Bond Wire

Figure 4 shows the electric potential in a bond wire after a grid refinement step. Regions with strongly varying gradient have been refined. Figure 5 shows a cut through the model with the amplitude of the corresponding current density. A magnification of the region around the right contact with current direction displayed is shown in Figure 6.

Figure 7 shows the running average of the inductance during five different computations. Figure 8 shows the corresponding standard deviation divided by the running average. This value becomes stable after $\approx 50,000$ iterations.

The corresponding error estimate is shown in Figure 9. 150,000 iterations take 220 secs time. The final result is given with 2 percent accuracy. A result with 5% accuracy is already obtained after 25,000 iterations, i.e. after 35 secs.

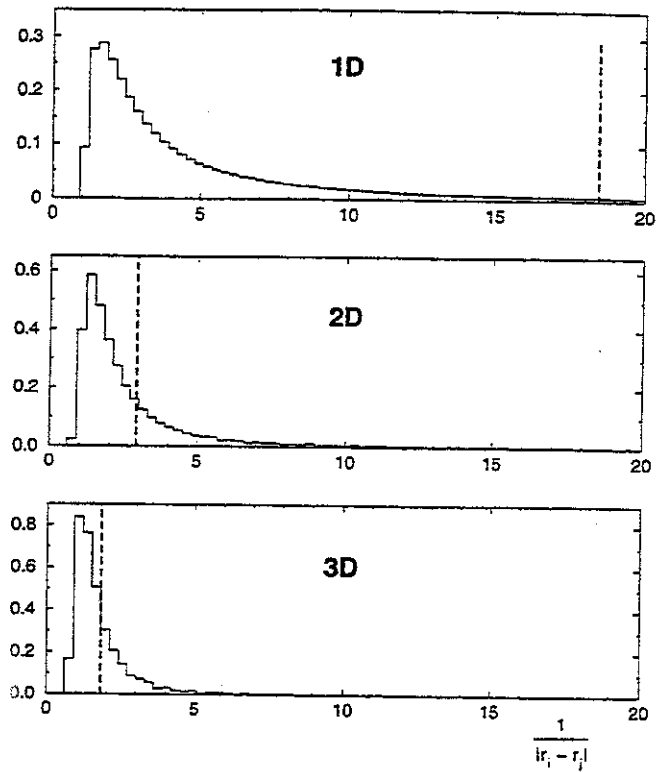


Figure 3: Distribution of values $1/|r-r'|$ on a line with length 1 (1D), on a square shaped surface with area 1 (2D), and on a cube with volume 1 (3D). For the computation of the distributions in each case $\approx 250,000,000$ terms were taken into account. Locations r and r' were taken from regularly distributed coordinates. The distributions are normalized. The expectation value of every distribution is marked with a dashed line.

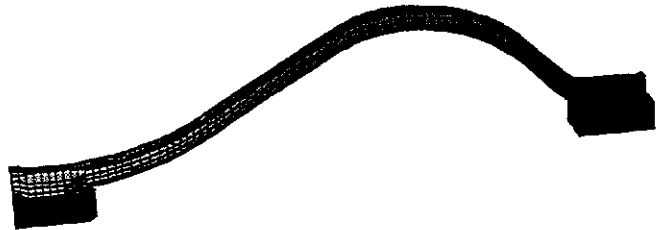


Figure 4: Electric potential in a bond wire model. The grid was adaptively refined.

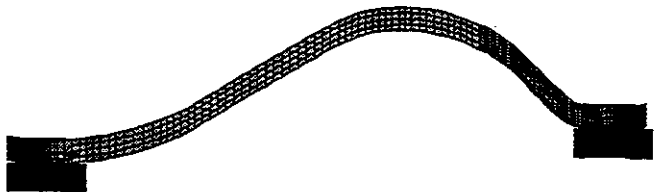


Figure 5: Cut through model of bond wire in 4. Here the magnitude of the current density is shown.

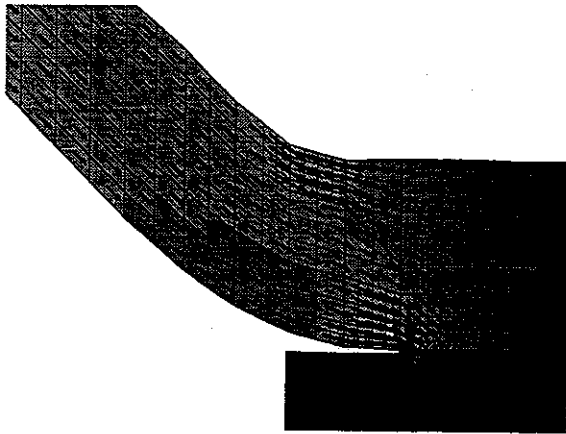


Figure 6: Magnification of area around the right contact in Figure 5 and direction of current density distribution.

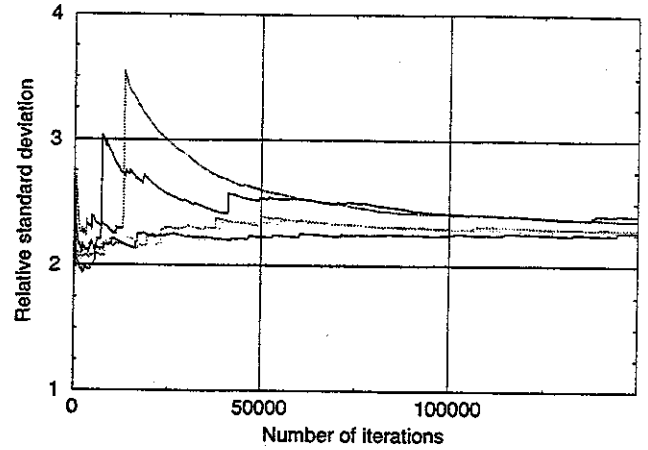


Figure 8: Standard deviation divided by the running average (Figure 7). Used for computation of an error estimate.

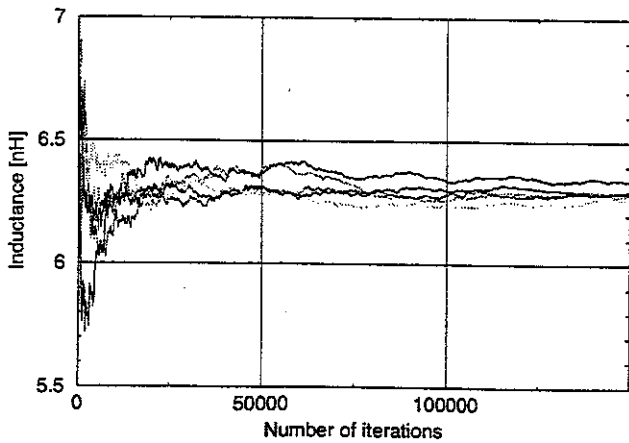


Figure 7: Running average of inductance during Monte Carlo sampling. Five different computations are shown.

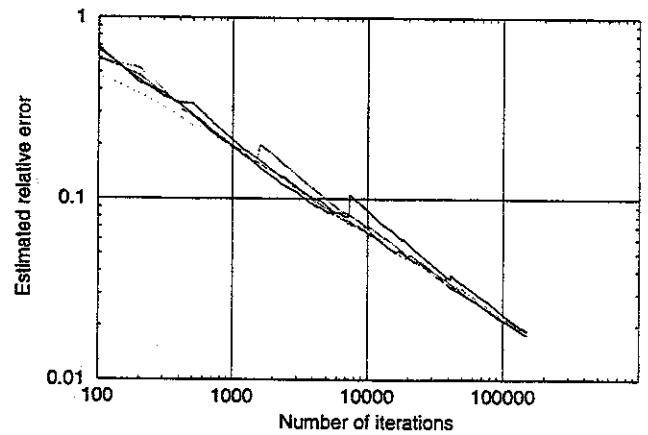


Figure 9: Running error estimates (relative error) for inductance values shown in Figure 7

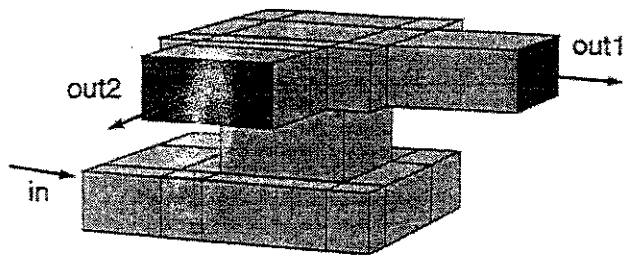


Figure 10: Structured grid model of a via. Grid lines intersect vertically. Electric contacts are also shown.

Comparison with Fasthenry

The algorithm of Fasthenry has been published in [1]. Fasthenry models are constructed following the procedure published in [5]. Constraints of Fasthenry are its brick shaped elements and that bricks cannot overlap when they are inclined at an angle other than 90 degrees. This is why the bondwire shown in the preceding section could not be modeled with Fasthenry without a change of the geometry.

The comparison is carried out with the via structure shown in Figure 10. In order to compare the methods for different model sizes, this grid has been refined by dividing every element into more elements all of equal size and shape. The number of divisions is indicated in Table 1. Values L_{11} , L_{22} and L_{12} denote the inductance of conductor 1, 2 and their inductive coupling respectively. Energy terms W_{ij} (3 are calculated with 1% accuracy).

Both methods give almost correct results for even the coarsest discretization of the model. In case of small models Fasthenry is a lot faster than the Monte Carlo code. But with increasing model size Fasthenry becomes slower and memory demand increases. Memory demand of the Monte Carlo code is much smaller for bigger models and the time break-even is reached at a model size of around 2.000 degrees of freedom.

Conclusion

It has been shown that the computation of the magnetic field energy of a given current distributions with Monte Carlo sampling can be used for inductance extraction for cases where the skin effect is negligible. The method is applicable for any given current density distribution. The convergence rate depends rather on the shape of geometries than on the number of grid elements. Convergence becomes slower for geometries with high aspect ratios and faster for cube shaped geometries.

Model sizes are limited by the amount of computer memory needed during the computation of current density distributions. This involves the solution of a sparse matrix equation only. During Monte Carlo sampling only the geometry and the current density information have to be stored in memory. This makes it possible to set up models with a much higher number of degrees of

freedom than possible with Fasthenry where Fasthenry also models the skin-effect.

REFERENCES

- [1] M. Kamon, M. J. Tsuk and J. White, "Fasthenry: A multipole-accelerated 3-d inductance extraction program", *IEEE Transactions on Microwave Theory and Techniques*, 42(9), 1750-1758, 1994
- [2] F. Grover, "Inductance Calculations", van Nostrand Co., 1946
- [3] R. Rubinstein, "Simulation and the Monte Carlo Method", J. Wiley & Sons, 1981
- [4] ISE Integrated Systems Engineering AG, "Solidis-ISE User Manual and Reference", ISE AG Zurich, 1997
- [5] A. Ruehli, "Equivalent Circuit Models for Three-Dimensional Multiconductor Systems", *IEEE Transactions on Microwave Theory and Techniques*, MTT-22(3), 1974

Solver	divisions	Deg. of freedom	L_{11}	L_{12}	L_{22}	Time	Mem.
fh	1	14	2.085	1.059	1.714	0.5	0
mc	1	84	1.904	9.647	1.506	s0.5 mc360	s0 mc3
fh	8	256	2.029	1.032	1.645	12	6
mc	8	399	1.957	9.976	1.576	s2 mc375	s8 mc3
fh	27	1026	2.0136	1.024	1.627	165	22
mc	27	1096	1.998	1.014	1.595	s6 mc368	s12 mc5
fh	64	2624	2.007	1.020	1.618	870	68
mc	64	2325	1.991	1.012	1.596	s12 mc377	s18 mc8
fh	125	5350	2.003	1.018	1.614	2518	136
mc	125	4236	1.987	1.012	1.601	s26 mc383	s29 mc13

Table 1: Comparison between Fasthenry (fh) and inductance extraction with Monte Carlo sampling (mc). The grid refinement, indicated by 'divisions', is different for every simulation. Degree of freedom in case of Fasthenry denotes the number of meshes in the Fasthenry-model. In case of the Monte Carlo solver degree of freedom denotes the size of the finite element matrix for computation of the electric potential. Time values are given in seconds. Memory demand is given in MB. Time and memory demand are given separately for the mc solver. Values of SOLIDIS-ISE are marked with an 's', values for the Monte Carlo solver are marked with 'mc'.